AD-A058 887 CALIFORNIA UNIV LOS ANGELES DEPT OF MATERIALS F/G 11/6
ON THE AMPLITUDE DISTRIBUTION OF BURST EMISSION DUE TO MNS INCL--ETC(U)
JUL 78 K ONO, R LANDY, C OUCHI N00014-75-C-0419
UNCLASSIFIED TR-78-03 NL

1 OF 1
ADA
058887

END
DATE
FILMED
11-78
DDC

LEVEL II

12

Technical Report No. 78-03

to the

Office of Naval Research

Contract No. N00014-75-C-0419

ON THE AMPLITUDE DISTRIBUTION OF BURST EMISSION DUE TO MnS INCLUSIONS IN HSLA STEELS

Kanji Ono and R. Landy
Materials Department
School of Engineering and Applied Science
Los Angeles, California 90024

and

C. Ouchi
Technical Research Center
Nippon Kokan K.K.
Kawasaki, Japan

July 1978

(14) TR-78-03

SECURITY CLASSIFICATION OF THIS PAGE (When Data Entered)

REPORT DOCUMENTATION PAGE	READ INSTRUCTIONS BEFORE COMPLETING FORM
1. REPORT NUMBER: ONR Technical Report No. 78-03	2. GOVT ACCESSION NO. / 3. RECIPIENT'S CATALOG NUMBER
4. TITLE (and Subtitle): On the Amplitude Distribution of Burst Emission due to MnS Inclusions in HSLA Steels	5. TYPE OF REPORT & PERIOD COVERED: Technical rept. / 6. PERFORMING ORG. REPORT NUMBER
7. AUTHOR(s): Kanji K. Ono, R. Landy and C. Ouchi	8. CONTRACT OR GRANT NUMBER(s): N00014-75-C-0419
9. PERFORMING ORGANIZATION NAME AND ADDRESS: Materials Department, 6531 Boelter Hall, University of California, Los Angeles, CA 90024	10. PROGRAM ELEMENT, PROJECT, TASK AREA & WORK UNIT NUMBERS: (12) 15p.
11. CONTROLLING OFFICE NAME AND ADDRESS: Physics Program, ONR-800 N. Quincy Street, Arlington, VA 22217	12. REPORT DATE: July 1978 / 13. NUMBER OF PAGES: 13
14. MONITORING AGENCY NAME & ADDRESS (if different from Controlling Office)	15. SECURITY CLASS. (of this report): Unclassified / 15a. DECLASSIFICATION/DOWNGRADING SCHEDULE
16. DISTRIBUTION STATEMENT (of this Report): Unlimited	DISTRIBUTION STATEMENT A Approved for public release; Distribution Unlimited
17. DISTRIBUTION STATEMENT (of the abstract entered in Block 20, if different from Report)	
18. SUPPLEMENTARY NOTES: To be presented at the 4th Acoustic Emission Symposium, Tokyo, Japan (Sept. 18-20, 1978), and published in the Proceedings Volume.	
19. KEY WORDS (Continue on reverse side if necessary and identify by block number): Acoustic Emission; Steel; Inclusion, Nonmetallic; Amplitude Distribution	
20. ABSTRACT (Continue on reverse side if necessary and identify by block number): See next page	

406 237

78 09 05 220

DD FORM 1 JAN 73 1473 EDITION OF 1 NOV 65 IS OBSOLETE
S/N 0102-LF-014-6601

SECURITY CLASSIFICATION OF THIS PAGE (When Data Entered)

ON THE AMPLITUDE DISTRIBUTION OF BURST EMISSION DUE TO MnS INCLUSIONS IN HSLA STEELS*

by

K. Ono, R. Landy and C. Ouchi+
Materials Department
School of Engineering and Applied Science
University of California
Los Angeles, California 90024

ABSTRACT

It is well known that the ductility of a steel plate, particularly in the thickness (short transverse) direction, is sensitive to the number, size, shape and distribution of nonmetallic (primarily MnS) inclusions. In this study, AE behavior was correlated to several inclusion parameters, varied by rolling mill practices and different sulphur levels in the steel used. Burst-type AE signals were observed in the thickness direction samples. Their numbers and intensity increased with the sulphur content, and also depended on the rolling ratio and finish rolling temperature. The origin of burst emission was established as the decohesion of flattened MnS inclusions. Amplitude distribution of AE signals was describable by a Weibull distribution. It was also found that the size distribution of MnS inclusions takes an identical form. The two independently determined distributions were correlated by considering the stored elastic strain energy at an inclusion and of the transducer response to mechanical pulse excitation. To explain stress dependence of AE amplitude distribution, the size dependence of decohesion probability was also introduced.

* Acoustic emission

* Supported by the ONR Physics Program

+Technical Research Center, Nippon Kokan, K.K.
Kawasaki, Japan

A

Introduction

The number, size, shape and distribution of nonmetallic inclusions affect the ductility of a high strength, low alloy (HSLA) steel plate, particularly in the thickness (short transverse) direction[1,2]. Of several types of inclusions, the behavior of MnS inclusions is often crucial in determining the mechanical properties of the plate, since they can be flattened to thin ribbon shapes during hot rolling operation[3,4]. It is, therefore, important to understand the response of these inclusions to mechanical loading, which results in the elastic and plastic deformation of the steel matrix.

Acoustic emission (AE) has proved to be a useful tool in detecting the decohesion and fracture of MnS inclusions in steel[5-7]. Our previous studies correlated these processes to burst-type AE observed during tensile testing of an HSLA steel in the through-thickness (Z) direction. The number of burst AE increased with the sulphur content. When tensile samples of the same steel were tested in the longitudinal (L) or transverse (T) direction, only continuous-type AE was produced, and the intensity was independent of the sulphur content. Samples in the L or T direction produced significant AE activities only during initial yielding (or during Lüders elongation). During compression testing of the L direction samples, the intensity of AE signals was essentially identical to that in tension; i.e., no effect on AE from changes in the loading direction. In contrast, the loading direction produced a large change in AE behavior in the Z direction samples. Showing completely different AE behavior from that observed in tension, a compression sample along the Z direction behaved indistinguishably from that of the L direction, producing only continuous AE during the Lüders elongation.

In order to understand the behavior of the MnS inclusions, stress concentrations in and around the inclusions need to be evaluated. Recently, Shibata and Ono[8,9] considered internal stresses in and around an oblate spheroidal inclusion-matrix boundary. The results were adopted to consider an MnS inclusion in steel[7,8]. It was found that the observed AE behavior as a function of the loading orientation and direction is consistent with the predicted stress concentrations. The calculation indicated that a stress of 200 to 300 MPa initiates the decohesion at the broad face of the MnS-steel interface for the Z direction sample in tension. As the decohesion may initiate from both faces on opposite sides of an inclusion, fracture perpendicular to the inclusion face necessarily accompanies the process. The decohesion at the interface has been observed in situ in a scanning electron microscope[10].

In this study, we have evaluated the number and amplitude distribution of burst-type AE and related them to quantitatively characterized parameters of MnS inclusions in five different HSLA steel plates. These inclusion parameters were varied by rolling mill practices and two different sulphur levels in the steel used. It was found that the amplitude distribution of AE signals and the size distribution of MnS inclusions take an identical form and are describable by a Weibull function. The two independently determined distributions were correlated by considering the stored elastic strain energy and the transducer response to mechanical pulse excitation. The later subject will be elaborated below, followed by experimental findings and discussions.

Transducer Response

When a mechanical stimulus excites a resonant-type AE transducer, the electrical signal generated by the transducer can be approximated by a damped sinusoid. Harris et al.[11] introduced this approximation and later experiments have confirmed its validity. Most recent experiments for the evaluation of transducer response have employed the fracture of a fine pencil lead or a fine glass tubing. The impulse response of the transducer, r(t) is then expected to be

$$r(t) = e^{-\beta t} \cdot e^{i\omega_o t} \cdot u(t) \tag{1}$$

where t is time, β is a decay constant, $i^2 = -1$, $f_o = \omega_o/2\pi$ is the resonance frequency and u(t) is the unit step function, i.e., $u(t) = 1$ for $t > 0$ and $u(t) = 0$ for $t \leq 0$. The frequency response of the transducer, F(f), is given by the Fourier transform of r(t) and is

$$F(f) = [2\pi i(f - f_o) + \beta]^{-1} . \tag{2}$$

Hence, at frequencies at $f = f_o \pm \beta/2\pi$, one obtains $F(f) = F(f_o)/\sqrt{2}$; that is the bandwidth at 3 dB down is given by β/π.

Suppose a mechanical stimulus on the transducer can be represented by a rectangular pulse with magnitude S and duration T. The stimulus s(t) can be expressed as

$$s(t) = S[u(t) - u(t - T)] \tag{3}$$

The transducer response R(t) to this stimulus is given by the convolution of s(t) and r(t); that is,

$$R(t) = \int_{-\infty}^{\infty} s(\lambda)\, r(t - \lambda)\, d\lambda . \tag{4}$$

Upon integration, one obtains for $0 \leq t \leq T$,

$$R(t) = \frac{S}{\beta - i\omega_o} [1 - e^{-\beta t} \; e^{i\omega_o t}] \tag{5a}$$

and for $t > T$,

$$R(t) = \frac{S(e^{\beta T} - i\omega_o - 1)}{\beta - i\omega_o} \; e^{-\beta T + i\omega_o t} . \tag{5b}$$

When T becomes small compared to $1/\beta$, Eq. (5b) tends to approach the impulse response or Eq. (1). When $t = T$, the envelope of R(t) reaches maximum. For a small T, the magnitude of this maxiumum output is proportional to T, since

$$R_{max} = R(T) = \frac{S(1 - e^{-\beta T + i\omega_o T})}{\beta - i\omega_o} = S \cdot T \tag{6}$$

This result leads to an interesting consequence, as the maximum value of the envelope of R(t), R_{max}, in fact, corresponds to the peak amplitude of a burst emission signal, V_p.

Before proceeding further, we present results of a simulation experiment. Here, the mechnical stimulus was replaced by an electrical pulse generator, producing rectangular pulses (magnitude: 1 V, repetition rate: 500 Hz and pulse duration: 0.08 to 1.0 μs). The transducer response was simulated by a bandpass filter (ω_o = 2.86 MHz, β = 5 kHz). The peak voltage of filter output was measured on an oscilloscope. Results are shown in Fig. 1, where the peak voltage V_p increases linearly with the pulse duration T. This is in accord with Eq. (6).

The energy of the mechanical stimulus is given by

$$E_s = \int_{-\infty}^{\infty} s^2(t)\, dt = S^2 T \tag{7}$$

where s(t) is assumed to represent the surface displacement or velocity. Two cases are of particular interest.

Case 1. The pulse duration is constant and the pulse height varies.

$$E_s \propto S^2 \propto (R_{max})^2 = V_p^2 \tag{8}$$

Case 2. The pulse height is constant and the pulse duration varies.

$$E_s \propto T \propto R_{max} = V_p \tag{9}$$

In previous studies of AE, Case 1 has been taken for granted[11]. The above analysis shows that the proportionality between E_s and V_p^2 holds only when all the events have an identical pulse duration. Unless this condition is met the oft-quoted relation of Eq. (8) cannot be justified. Case 2 is a surprizing result, even though it applies only to small values of T. However, the conditions of constant S and changing T are physically realizable with a number of AE source mechanisms.

Experimental Procedures

Materials and Properties

Starting materials were two slabs of Al-killed BOF steels, having the nominal composition of 0.16 C, 0.3 Si, 1.3 Mn, 0.016 P, 0.02 Nb, 0.025 Al and 0.005N. Slab A, having 0.019 S and 160 mm initial thickness, was rolled to either 120 mm or 25 mm with the finish rolling temperature of 1000°C. These are designated as T1, T2, and T3, respectively. Slab B had 0.006 S and reduced from 190 mm to 25 mm thickness with the finish rolling temperature of either 1000°C (T4) or 750°C (T5). Initial temperature was 1200°C in all cases. All the plates were finally normalized at 900°C for 1 hr. The ranges of tensile properties for the Z direction were: Yield Strength = 368 - 387 MPa; Tensile Strength = 458 - 523 MPa; Elongation = 4 - 25%.

Fig. 1. Peak ouput voltage of a bandpass filter V_p against the duration of input pulse T.

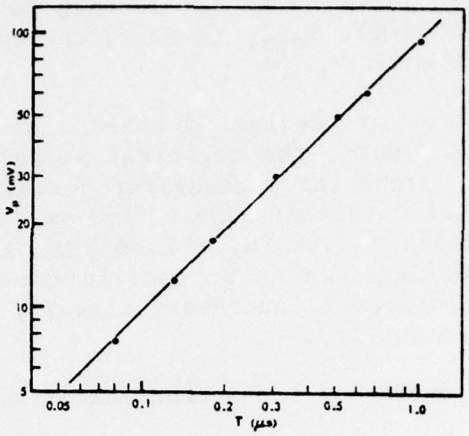

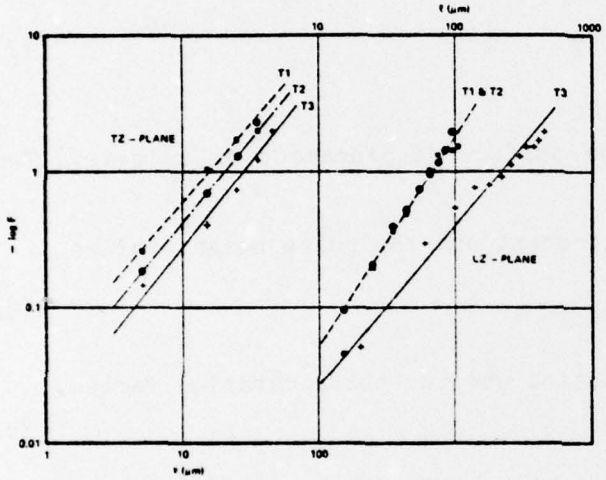

Fig. 2. Cumulative distribution of MnS inclusion against their length on LZ and TZ planes for steels T1, T2 and T3.

TABLE 1. MnS Inclusion Distribution

	LZ-Plane				TZ-Plane			
	$\bar{\ell}$ (μm)	$\bar{n}$ (cm^{-2})	a	m	$\bar{\ell}$ (μm)	$\bar{n}$ (cm^{-2})	a	m
T1	56	7.5×10^{3}	6.9×10^{-4}	1.53	16	9.0×10^{3}	1.4×10^{-2}	1.28
T2	64	5.3	6.9×10^{-4}	1.53	22	8.3	1.0×10^{-2}	1.27
T3	160	7.7	1.0×10^{-3}	1.13	30	12.7	6.5×10^{-3}	1.29
T4	120	3.2	9.6×10^{-4}	0.72	21	3.2	3.1×10^{-2}	1.52
T5	180	2.0	3.2×10^{-4}	0.90	26	3.0	1.4×10^{-4}	0.98

Inclusion analysis was performed via standard metallographic technique at 400X magnification using at least 60 fields per sample. No differentiation between inclusion types was made during inclusion counting, although it was noted that sulfide inclusions predominated.

Test Procedure

Tensile tests of the Z direction samples were performed using a floor-model Instron at 23°C. Nominal strain rate was 1.1×10^{-3} s^{-1}. Tensile samples in the Z direction were prepared by friction welding of two steel rods, followed by machining. The shape of the samples was basically a half-size ASTM round tensile specimen (6 mm diameter, 40 mm reduced section length), but the center section had a reduced diameter 4.5 mm over 19 mm long portion. This shape eliminated undesirable deformation outside the gauge section.

AE tests utilized a wideband sensor fabricated from a PZT-5 element (compressional mode, 3 MHz fundamental frequency, 6.3 mm diameter). It was mounted at the end of a round tensile sample with viscous resin. A preamplifier with a 30 to 2,000 kHz bandpass filter plug-in (Model 160, Acoustic Emission Tehnology Corp. (AETC), Sacramento, Calif.), a signal processor (model 201, AETC), video tape recorder (Sony AV-3650, modified by AETC for AE signal recording) and an instrumentation tape recorder (Bell and Howell, VR 3700A) were utilized. The input noise level was 3.2 μV. Amplitude distribution analysis of AE events utilized a dedicated analyzer (Model 203, AETC), employing a resonant transducer (AC 175L, AETC) and a preamplifier with a narrow passband of 125 to 250 kHz. The input noise level for this set-up was 1.2 μV. AE event counts were also obtained using the amplitude distribution analyzer and recorded separately. The threshold level was set at six to eight times the background noise level.

Results

Microstructures of the steel plates consisted of ferrite-pearlite mixtures. Banded structures developed in plates T3, T4 and T5. Ferrite grain size was 9 to 11 μm and the fraction of pearlite was 0.15 to 0.18. In heavily rolled plates, MnS inclusion exhibited extensive stretching along the rolling direction. Average inclusion size ($\bar{\ell}$) and number per unit area, ($\bar{n}$), measured on the LZ and TZ planes are given in Table 1. The lower limit of inclusion size in the measurements was about 2 μm. Fractional cummulative distribution of inclusion size, $D(\ell)$, for each of the five plates was obtained by counting the number of inclusion grater than a particular size. The observed data fit the following relation quite well;

$$D = \exp(-a\,\ell^m) \tag{10}$$

where ℓ is the inclusion size in μm and a and m are constants. By plotting log D against ℓ in a log-log plot, the validity of Eq. (10) is demonstrated by the straight line fit in Fig. 2. Constants derived are given in Table 1.

Typical AE activities during tensile testing of a Z direction sample are shown in Fig. 3. During the initial part of deformation, AE activities were high, but persisted at lower levels until the maximum load was reached. AE

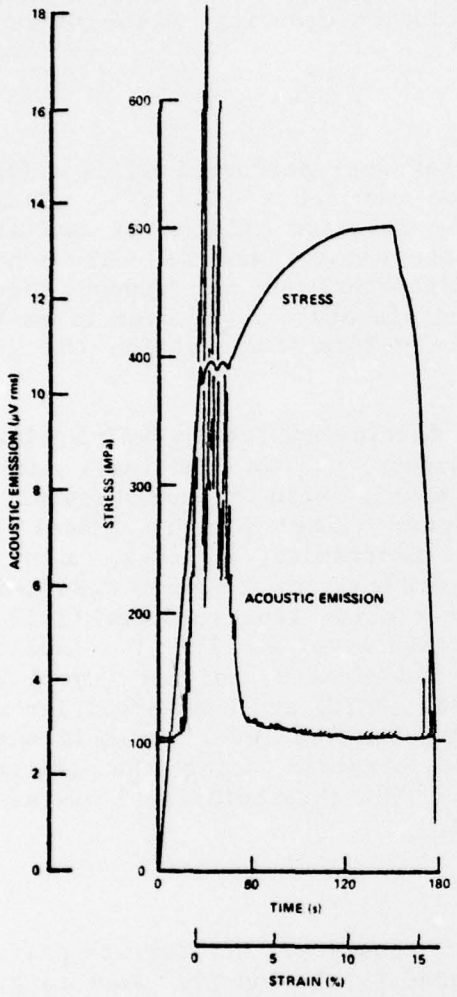

Fig. 3. Stress and AE level against strain or time for tensile test of the Z direction sample of steel T5.

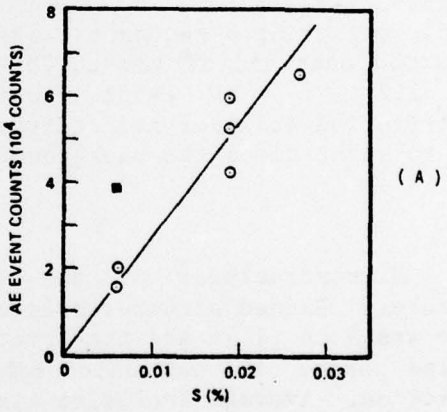

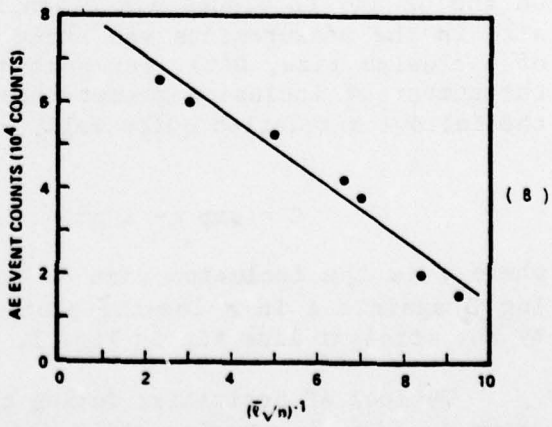

Fig. 4. (a) Total AE event counts of the Z direction samples versus sulphur content of five steel plates plus two plates previously reported. (Threshold voltage = 20 μV) Filled square indicates the datum point for control rolled plated (T5). (b) Total AE event counts as in (a) against inclusion factor, $(\ell \sqrt{n})^{-1}$.

signals started to increase at 30 to 40% of the yield stress. Pre-yield AE activities varied among five steel plates and also depended on the strain rate. When a T3 sample was tested at 2.22×10^{-4} s^{-1}, only 5% of the total AE events occurred before the upper yield point. When another sample of the same steel (also the Z direction) was deformed at one-fifth of the rate, 60% of the total AE events was recorded before reaching the 0.2% yield stress, σ_y (no discontinuous yielding for this sample). In the latter, AE event counts increased with the 3.5 power of applied stress over the range of 0.3 to 1.1 σ_y.

Relative magnitude of AE activities was compared quantitatively by integrating V_r over time and by total counts. The values of V_r were corrected for the background noise level. Since the ductility of T3 samples was limited, the above parameters were also evaluated at 5% strain. Results are summarized in Table 2 and clearly demonstrate that AE activities increase with increasing amounts of hot rolling in a given steel. For the plates with similar rolling conditions (T3 and T4), higher AE activities correspond to a higher sulphur content. When controlled rolling procedure was used (plate T5), more AE was produced in comparison to plate T4 with identical composition and rolling ratio, but with a higher finish rolling temperature.

In Fig. 4a, the total AE event counts N_e are plotted against the sulphur content. This plot includes data from two plates used in our previous studies, although the rolling and heat treatment conditions were slightly different. Except for the control-rolled plate (T5), a linear relationship provides a fair fit to data. This indicates an obvious trend of higher N_e for greater sulphur content.

Amplitude distribution analysis of burst-type AE was performed during tensile tests with frequent interruptions. Results for T3 steel samples are shown in Fig. 5. Typical amplitude distributions of a Z direction sample are given in Fig. 5a and can be represented by

$$F_e(V_p) = A \exp (- B V_p^q) , \qquad (11)$$

where F_e is the cumulative AE peak amplitude distribution, V_p is the peak voltage of an AE event and A, B and q are constants. Note that this is a form of the Weibull distribution and is identical to Eq. (10). Curve 1 in Fig. 5a was obtained at 82% of the yield stress (0.2% offset), Curve 2 at the yield stress, and Curve 3 at 120% of the yield stress, respectively. The exponent q basically determines the shape of F_e. It systematically varied during the tensile test of T3 sample. In the pre-yield range, q = 0.30 was found from 14 measurements. The value of q was 0.35 during the yield range and increased to 0.4 to 0.5 in the work-hardening region. The identical form of F_e was also observed in other samples. In a T5 steel samples, the observed range was slightly lower, resulting in the range of q = 0.25 to o.35 over the pre-yield to work-hardening regions. Observed amplitude distribution of an L direction sample (T3) is compared to that f a Z direction sample (T3) in Fig. 5b. Both were obtained during the Lüders elongation. The distribution for the Z sample had a q value of 0.3. The L sample produced only continuous-type AE, for which Eq. (11) with q = 4 gave the best fit.

TABLE 2. AE Data Summary

Steel	Integrated V_r (at 5%)	Integrated V_r (Total)	AE Events (10^3 counts) (at 5%)	AE Events (10^3 counts) (Total)
T1	26	36	41	42
T2	48	59	51	52
T3	57	57	59	59
T4	30	35	19	20
T5	55	56	37	38

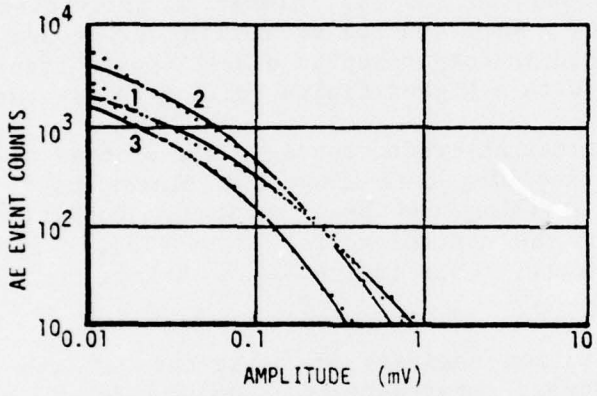

(A)

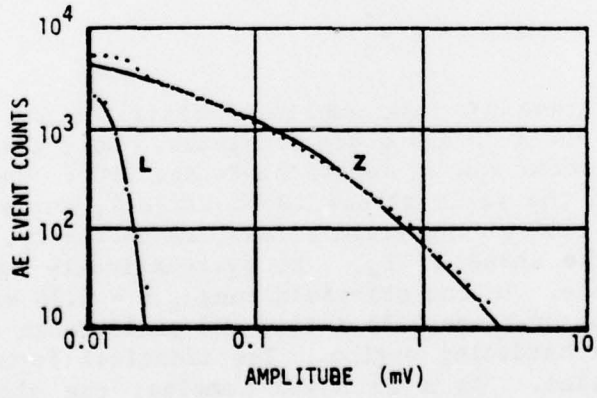

(B)

Fig. 5. Cumulative amplitude distribution of AE events during tensile tests of steel T3. (a) A sample in the Z direction ($\dot{\varepsilon} = 4.44 \times 10^{-5} s^{-1}$) 1. Stress level at 0.82 σ_y; 2. At σ_y; 3. At 1.2 σ_y. (b) During Lüders elongation of L and Z direction samples ($\dot{\varepsilon} = 2.22 \times 10^{-4} s^{-1}$). Data are fitted with Eq. (11) having q = 0.3 for Z and q = 4 for L, respectively.

The distribution from the Z sample often had deviations below 20 μV. The deviation appears to originated from the continuous AE signals, for it was most pronounced during the yielding and was either insignificant or absent in the pre-yield and work-hardening ranges.

Discussion

From a series of AE tests performed using well characterized ferritic-pearlitic steel plates, the following observations have emerged:

1. In tensile or compressive testing of steel samples in the longitudinal (or transverse) direction, only continuous-type AE signals are produced during the Luders elongations, the intensity of which is independent of the sulphur content. AE activities are very low in the work-hardening stage. This type of AE is due to the plastic deformation of ferrite and pearlite.

2. In tensile testing of steel samples in the thickness direction, burst-type AE is the primary feature from the pre-yield region to fracture. Peak activities occur at the initial yielding and at the beginning of work-hardening. The total intensity and the number of burst emission increase with increasing the sulphur content of steel. This type of AE originates primarily from the decohesion of MnS inclusions in steel.

In this study, we attempt to obtain quantitative correlations between the number and the peak amplitude distribution of burst-type AE and inclusion parameters. Generally, the number of AE events increases with the sulphur content, which is a measure of the volumetric content of MnS (See Fig. 4a). It is noted that good proportionality is found, when similarly proessed plates are compared. However, the control rolled sample (a filled square produced nearly twice the number of AE events of the conventionally rolled sample. For a given sulphur content (0.019% S), the number of observed AE events was higher with increasing rolling ratio.

It should be mentioned that the number of AE events correlates well with the inclusion factor, which was originally introduced by Hood and Jamieson.[12] It is defined here as $(\bar{\ell}\sqrt{\bar{n}})^{-1}$, and is the ratio of the average distance between inclusions to the average length of the inclusions. Figure 4b shows a plot of N_e against $(\bar{\ell}\sqrt{\bar{n}})^{-1}$. While the physical significance of this finding is not obvious, the inclusion factor has been shown to correlate well with such measures of ductility as the Charpy shelf energy, the strain and terminal speed of fracture propagation.[12] Thus, the present observation indicates that the number of AE events can be an empirical parameter of ductility.

Next, we want to compare the number of MnS inclusions to that of AE events. From the number of inclusions per unit area on two orthogonal planes, the number per unit volume <n> may be approximated by $\bar{n}_{LZ}\sqrt{\bar{n}_{TZ}}$ or $\bar{n}_{TZ}\sqrt{\bar{n}_{LZ}}$. Averaging the two values, we obtain the following:

steel	T1	T2	T3	T4	T5
<n>	7.5	5.4	9.9	1.8	1.2×10^5 cm^{-3}

The volume of the specimen was 0.30 cm^3. With the exception of plate T5, the observed AE events were 1/3 to 1/5 of the number of MnS inclusions. The <n> values for T5 appears to be underestimated and was comparablee to the number of AE events. The discrepancies can be traced to the presence of numerous events below the threshold voltage and to the limitation of the transducer sensitivity. Using T3 specimens with a more sensitive resonant transducer and 10 μV threshold (one-half of the previous setting), the total AE event counts of 1.83×10^5 and 1.39×10^5 were obtained for the strain rate of 2.22×10^{-4} s^{-1} and 4.44×10^5 s^{-1} respectively. These represent about a half of the observed number of the inclusions. Effect of strain rate appears to be insignificant, for these events originate from the the pre-existing inclusions. The inclusion size distribution data for this steel indicates that these AE events are produced by the inclusions of 40 μm or greater. The extrapolation of AE amplitude distribution data implies that the total AE event count should be at least doubled, in order to account for the sub-threshold events. When this correction is included, the total number of AE events become directly comparable to that of the observed inclusions.

Let us next consider the origin of the observed amplitude distribution. Since the decohesion of MnS inclusions has been established as the source of burst-type AE, the size distribution of these inclusions is expected to be the primary factor. When an inclusion separates from the matrix under stress, σ, the amount of elastic strain energy released, E_s, is of the order of $\sigma^2 \ell^3/2E$, where E is the Young's modulus and ℓ is the major diameter of the inclusion. Equation (10) can be written as

$$N = N_o \exp[- a(2E/\sigma^2)^{m/3} E_s^{m/3}] \quad , \tag{12}$$

where N is the number of the inclusions that release E_s or less upon decohesion and N_o is the total number of the inclusions. From Table 1, m is known to be 0.7 to 1.5 with the likely values of 0.9 to 1.2. Consequently, Eqs. (11) and (12) coincide if the E_s is proportion to V_p. This corresponds to Case 2 discussed earlier, for which the duration of transducer excitation is proportional to E_s. At present, the E_s-V_p proportionality cannot be verified directly by experiment. Yet, the agreement between two independently determined distribution functions is significant, for this is the first success in quantitatively explaining the observed AE amplitude distribution.

Another approach to compare the AE amplitude and inclusion size distributions is possible, using a semi-empirical linear relation between V_p and incremental crack areas, ΔA, derived by Desai and Gerberich[13]. Their relation was derived by a fracture-mechanical compliance analysis and by an experimentally observed relation between AE amplitude and load drop during

fracture testing of crack-line loaded or compact tension specimens. It should be viewed with caution, for the time of incremental cracking was not taken into account. Taking ΔA as ℓ^2, Eq. (10) yields the following:

$$N = N_o \exp(- a' V_p^{m/2}), \tag{13}$$

where a' is a constant. As m/2 ranges from 0.45 to 0.6, Eq. (13) predicts sharp decreases in N with respect to V_p, and fails to match the observed AE distributions with q values of 0.25 to 0.5. Thus, this approach appears to be unable to predict the observed amplitude distribution.

The observed increase in the q value as a function of applied stress or strain indicates that larger inclusions produce burst AE at lower stress levels and that they are depleted as applied stress is increased. This is expected, since the probability of decohesion of an inclusion is likely to be dependent on its size. The inclusion-matrix boundary probably contains defects, from which the decohesion is expected to initiate. This implies that length or area dependent probability of decohesion ($P\ell$ or P_a) needs to be included in the above consideration by multiplying $P\ell$ (or P_a) to the differential inclusion size distribution. When the length dependent term was included in the derivation of Eq. (13), the exponent (m/2) was reduced by about 0.1, although substantial deviations from the form of Eq. (11) became apparent. This reduction in the exponent was still inadequate, but the concept of size dependent decohesion makes the second approach less untenable.

Acknowledgements

The authors are grateful to the Office of Naval Research, Physics Program for financial support.

References

1. "Sulfide Inclusions in Steel", edited by J. J. de Barbadillo and E. Snape, Amer. S. Metals, Metals Park, Ohio, 1975.

2. D. V. Wilson, Metals Tech., 1975, vol. 2, pp. 8-20.

3. I. Kozasu and J. Tanaka, "Sulfide Inclusions in Steel", edited by J. J. de Barbadillo and E. Snape , pp. 286-308, Amer. Soc. Metals, Metals Park, Ohio, 1975.

4. T. J. Baker, "Sulfide Inclusions in Steel", edited by J. J. de Barbadillo and E. Snape, pp. 135-38, Amer. Soc. Metals, Metals Park, Ohio, 1975.

5. K. Ono, H. Hatano and G. Huang, "Proc. 8th World Conf. on Nondestructive Testing", Section 3K, paper No. 3K3, Cannes, France, Sept., 1976, published by Conference Secretariat, Paris, France, 1976.

6. K. Ono, G. Huang and A. Kawamoto, "Internal Friction and Ultrasonic Attenuation in Solids", edited by R. R. Hasiguti and N. Mikoshiba, pp. 829-34, Univ. of Tokyo Press, Tokyo, Japan, 1977.

7. K. Ono, M. Shibata and M. A. Hamstad, Met. Trans. A (to be published).

8. M. Shibata and K. Ono, Acta Met. 1978, vol. 26, pp. 921-32.

9. M. Shibata and K. Ono, Materials Sci. and Engr., 1978, Vol. 34, pp. 131-37.

10. W. Roberts, B. Lehtinen and K. E. Easterling, Acta Met., 1976, vol. 24, pp. 745-58.

11. D. O. Harris, A. S. Tetelman and F. A. Darwish, "Acoustic Emission" ASTM-STP-505, edited by R. G. Liptai et al., pp. 238-49, Amer. Soc. Testing and Materials, Philadelphia, Penn., 1972.

12. J. E. Hood and R. M. Jamieson, J. Iron Steel Int., 1973, vol. 211, pp. 369-73.

13. J. D. Desai and W. W. Gerberich, Engr. Fracture Mech., 1975, vol. 7, pp. 153-65.